1-Amino-3-nitroguanidine (ANQ) in High-performance Ionic Energetic Materials

Niko Fischer, Thomas M. Klapötke and Jörg Stierstorfer

Department of Chemistry, Energetic Materials Research, Ludwig-Maximilian University of
Munich, Butenandtstr. 5 – 13 (Haus D), D-81377 Munich, Germany

Reprint requests to Prof. Dr. Thomas M. Klapötke. Fax: (+49-(0)89-2180 77492).
E-mail: tmk@cup.uni-muenchen.de

Dedicated to Professor Wolfgang Beck on the occasion of his 80th birthday

1-Amino-3-nitroguanidine (ANQ, **2**) was synthesized *via* hydrazinolysis of nitroguanidine (**1**). An appropriate Lewis structure of ANQ is drawn based on VB calculations. Due to its basicity, it can be protonated by strong mineral acids or acidic heterocycles. In order to synthesize new energetic materials the nitrate (**3**) and perchlorate (**4**) salts of 1-amino-3-nitroguanidine were synthesized by protonation of **2** with 40 % nitric acid and 60 % perchloric acid, respectively. 5-Nitrimino-1,4*H*-tetrazole obtained by reacting 5-amino-1*H*-tetrazole with 100 % HNO_3 was used to synthesize the nitriminotetrazolate salt **5**. Furthermore, the dinitramide salt **6** of 1-amino-3-nitroguanidine was synthesized by metathesis reaction of silver dinitramide and 1-amino-3-nitroguanidinium chloride. The dinitroguanidinate salt **7** was synthesized by protonation of **2** with 1,3-dinitroguanidine, which was prepared from nitroguanidine in anhydrous nitric acid/N_2O_5. All compounds were fully characterized by single-crystal X-ray diffraction, vibrational spectroscopy (IR and Raman), multinuclear NMR spectroscopy, mass spectrometry, elemental analysis, and DSC measurements. The heats of formation of **2 – 7** were calculated using the atomization method based on CBS-4M enthalpies. With these values and the experimental (X-ray) densities several detonation parameters such as the detonation pressure, velocity, energy, and temperature were computed using the EXPLO5 code. In addition, the sensitivities towards impact, friction and electrical discharge were tested using the BAM drophammer, friction tester as well as a small-scale electrical discharge device. A Koenen test with 1-amino-3-nitroguanidinium nitrate (**3**) was carried out in order to evaluate its explosive performance and shipping classification.

Key words: Nitroguanidine, Energetic Materials, Crystal Structure, Sensitivity

Introduction

The guanidine building block is one of the first structural moieties that has been known to the chemical and biological community and was discovered as early as 1866, when the first guanidine derivative was prepared by Hofmann [1]. Since then, guanidine chemistry has evolved into an extremely wide ranging field of applications starting from bioorganic chemistry and biochemistry [2] to inorganic chemistry, which most importantly can be traced back to a vast variability of derivatization of the guanidine moiety itself. If focusing on the field of inorganic chemistry, principally amination and nitration products of guanidine and the guanidinium cation are of major interest. Whereas the full series of amination products of the guanidinium cation (amino-, diamino- and triaminoguanidinium cation) is known [3], only mononitro- [4] and dinitroguanidine [5] as the respective nitration analogs have been discovered. On the one hand, amination of one of the amino groups in the guanidine moiety is achieved in a hydrazinolysis reaction, which can be applied up to three times leading to triaminoguanidine [3]. On the other hand, nitration is performed by treating guanidinium nitrate with conc. sulfuric acid. Nitroguanidine (**1**), $HN = C(NH_2)NHNO_2$, was first prepared in larger quantities by Jousselin [4] using the aforementioned synthetic pathway, when the compound separated upon dilution with water. However, for the preparation of dinitroguanidine, harsher conditions using N_2O_5 as nitration reagent are required [5]. (Mono)nitroguanidine
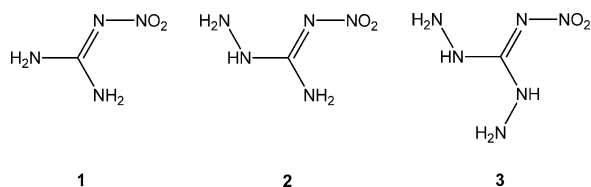
Fig. 1. Formula structures of amino-nitroguanidines: **1**: 1-nitroguanidine (NQ), **2**: 1-amino-3-nitroguanidine (ANQ), **3**: 1,3-diamino-5-nitroguanidine (DANQ) (not known yet).

is used principally as an ingredient in explosive and propellant formulations [6]. In this work, we mainly focus on a mixed amination/nitration product, which is aminonitroguanidine (**2**) and ionic materials, which utilize the aminonitroguanidinium cation as the respective protonated species. To date, only very little correspondence on aminonitroguanidine [7 – 9], especially if it comes to its structural investigation, is found in the literature. The next step in the preparation of mixed aminonitroguanidines could be the synthesis of diaminonitroguanidine (**3**), which still is a completely unknown field (Fig. 1).

To tie in with the application of nitroguanidine as an energetic material, the possible advantage resulting from introducing one further amino group to nitroguanidine is the generation of a larger gas volume when the compound is burned, which mainly is desired if the material is used in propellant systems. Apart from that, we also expect a higher heat of formation, which is a desirable feature if the compound should find application as a high explosive. Since one of the main topics in this work is the preparation of energetic aminonitroguanidinium salts, from the chemical point of view it is necessary to look at the acid base properties of mixed aminonitroguanidines. The introduction of one further amino group to nitroguanidine through a hydrazinolysis reaction has on the one hand the advantage of lowering the pK_B value of nitroguanidine so that it can be protonated in aqueous solution and therefore utilized as an energetic cation. However, we found that strong acids are required to protonate it. On the other hand, a second reason which makes 1-amino-3-nitroguanidine a suitable precursor in the synthesis of ionic energetic materials is its higher oxygen content compared to amino-substituted guanidine derivatives such as aminoguanidine or triaminoguanidine. It therefore combines the advantages of ease of protonation of the amino-substituted guanidine derivatives and good oxygen balances and high densities of

the nitro-substituted guanidine derivatives. Here we report on the synthesis and characterization of energetic salts of 1-amino-3-nitroguanidine such as the nitrate (**3**), the perchlorate (**4**), the nitriminotetrazolate (**5**), the dinitramide (**6**), and the dinitroguanidinate (**7**).

## Results and Discussion

Synthesis

Aminonitroguanidine (**2**) was synthesized in aqueous solution employing a hydrazinolysis reaction of commercially available nitroguanidine (**1**), whereas it is important to control the temperature accurately (Scheme 1) [7]. The product itself shows fairly poor solubility in water and therefore can be recrystallized from hot water.

Considering that the yield is only 45 %, there still is the question about the remaining starting material. Henry, Lewis and Smith [8], when reinvestigating the hydrazinolysis of nitroguanidine found two by-products of the reaction to be aminoguanidine and diaminoguanidine. Assuming an addition-elimination mechanism, nitroguanidine reacts with hydrazine to form an intermediate containing a tetrasubstituted carbon atom (**A**), which under the elimination of ammonia converts into **2**. However, the elimination of nitramine (which decomposes to N_2O and H_2O) leads to aminoguanidine **B**. The formation of diaminoguanidine as the second by-product can be explained by a further reaction of **2** with an additional equivalent of hydrazine to form species **C**, which under the elimination of nitramine forms diaminoguanidine **D** (Scheme 2) [10]. These findings are also corroborated by an experiment using a larger excess of hydrazine hydrate (2.2 eq.) in order to form diaminonitroguanidine, which only resulted in the isolation of **2** in minor yields (23 %).

For the synthesis of the ionic compounds, ANQ can be protonated by strong mineral acids such as hydrochloric acid, nitric acid and perchloric acid in excess at elevated temperatures (60 °C). During the syn-
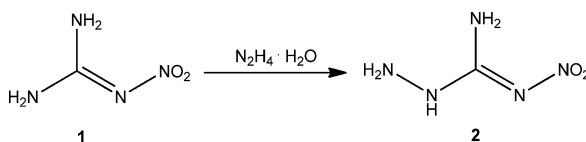
Scheme 1. Hydrazinolysis of nitroguanidine. Reaction conditions: stirring, 55 °C, 15 min.
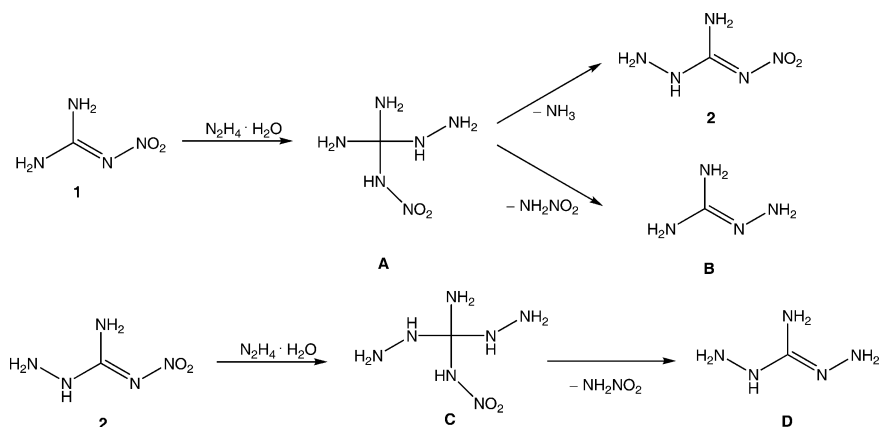
Scheme 2. Possible formation of the reaction by-products **B** and **D** assuming an addition-elimination mechanism.

thesis and crystallization of the nitrate (**3**) and the perchlorate (**4**) salt it is necessary to use acids of concentrations not lower than 40 % to avoid the precipitation of the poorly water soluble unprotonated ANQ. Once ANQ is dissolved in the corresponding acid, the nitrate or perchlorate salt will crystallize from the aqueous solution in large colorless blocks. Also the acidity of 5-nitriminotetrazole [11] is high enough to protonate aminonitroguanidine. The experiment was carried out under the same conditions using the sister compounds 1-methyl-5-nitriminotetrazole [11] and 2-methyl-5-nitriminotetrazole [11]. Both compounds failed to react, so that only aminonitroguanidine and the free acids could be isolated afterwards. The acidity of 5-nitriminotetrazole drops by adding an alkyl side chain to the heterocycle in such a way, that it is not sufficiently acidic any more to protonate aminonitroguanidine in aqueous solutions. For the preparation of the dinitramide a metathesis reaction using silver dinitramide [12] and the aminonitroguanidine hydrochloride salt is necessary. Aminonitroguanidinium chloride was synthesized by simple protonation of the ANQ unit with half-concentrated hydrochloric acid (20 % w/v).

The silver dinitramide was prepared according to the literature [12] as acetonitrile adduct, dissolved in very little acetonitrile and then added to an aqueous solution of aminonitroguanidinium chloride. To avoid the inclusion of one equivalent of silver coordinated to aminonitroguanidine, both, the hydrochloride and the silver dinitramide were reacted in equimolar amounts, whereas the silver dinitramide, dissolved in acetonitrile, was added dropwise to the solution of the hy-

drochloride in water. To ensure the completeness of the reaction, the mixture was further heated to 35 °C for 2 h under the exclusion of light resulting in the formation of **6** before being filtered off. From a facile Brønsted acid base reaction of an aqueous solution of **2** with an aqueous solution of dinitroguanidine the ionic product **7** could be isolated. It crystallizes directly from the reaction mixture with two and a half molecules of water per molecular unit. Dinitroguanidine was synthesized according to literature [5]. Interestingly, the exchange of one amino group in **2** by a nitro group lowers the pK_a value of the compound by a step which is just large enough to protonate **2** in aqueous solution. All reaction pathways are gathered in Scheme 3.

*Single-crystal X-ray structure analyses*

Experimental details

The low temperature (173 K) determination of the crystal structures of **2**–**7** was performed on an Oxford Xcalibur3 diffractometer with a Spellman generator (voltage 50 kV, current 40 mA) and a KappaCCD detector with a wavelength of 0.71073 Å. The data collection and reduction was carried out using the CRYSALISPRO software [13]. The structures were solved either with SHELXS-97 [14a] or SIR-92 [14b], refined with SHELXL-97 [15] and finally checked using the PLATON [16] software integrated in the WINGX [17] software suite. The non-hydrogen atoms were refined anisotropically, and the hydrogen atoms were located and freely refined. The absorptions were corrected with a Scale3 Abspack multi-scan method. Selected
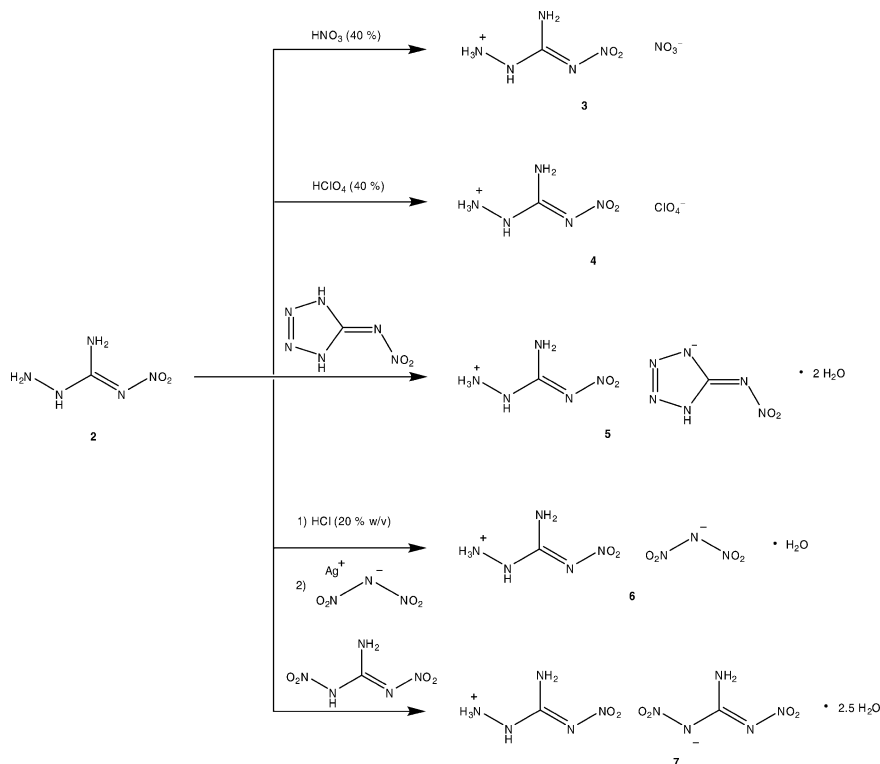
Scheme 3. Formation of aminonitroguanidinium salts **3 – 7**.

Structural details

Although compound **2** has been known for a long time, its crystal structure has never been published. Naidu *et al.* [19] claimed that ANQ belongs to a tetragonal crystal system which could not be confirmed in our study. Suitable single crystals of **2** were obtained from acidic aqueous media (40 % HF in H$_2$O). Compound **2** crystallizes in the monoclinic space group $P2_1/c$ with four molecules in the unit cell. The structure could sufficiently be refined using a merohedral twinning matrix. Fig. 2 represents the asymmetric unit. The bond lengths of neutral **2** and its protonated species **3 – 7** are listed in Table 2. Protonation always takes place at the outer hydrazine nitrogen atom N4, which does not influence the molecular structures (bond lengths and angles). All of the C–N bonds are
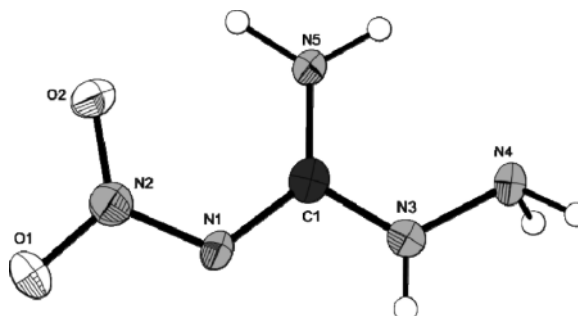
Fig. 2. Molecular structure of compound **2**. Ellipsoids are drawn at the 50 % probability level.

significantly shorter than C–N single bonds. Except for **2**, in all structures investigated in this work the C1–N5 distances are found to have the shortest values within the ANQ moieties. Also both N–N distances (N1–N2 and N3–N5) are between N–N single (1.48 Å) and N=N double (1.30 Å) bonds.

The relatively high density of 1.72 g cm^{-3} is a consequence of several strong N–H···N and N–H···O hy-

Table 1. Crystal structure data for compounds **2**–**7**.

	2	3	4	5	6	7
Formula	$CH_5N_5O_2$	$CH_6N_6O_5$	$CH_6N_5ClO_6$	$C_2H_{11}N_{11}O_6$	$CH_8N_8O_7$	$C_2H_{13}N_{10}O_{8.5}$
M_r	119.08	182.10	219.54	285.18	244.12	313.19
Cryst. size, mm^3	$0.08 \times 0.12 \times 0.22$	$0.18 \times 0.19 \times 0.20$	$0.13 \times 0.16 \times 0.20$	$0.19 \times 0.20 \times 0.29$	$0.09 \times 0.17 \times 0.18$	$0.16 \times 0.19 \times 0.32$
Crystal system	monoclinic	triclinic	triclinic	monoclinic	monoclinic	triclinic
Space group	$P2_1/c$	$P\bar{1}$	$P\bar{1}$	$P2_1/c$	$P2_1/c$	$P\bar{1}$
a, Å	6.8301(9)	7.1184(5)	7.1838(6)	9.3828(6)	7.3698(4)	7.2535(6)
b, Å	9.4491(14)	7.1485(6)	7.7952(8)	6.4467(4)	13.7548(8)	8.4153(7)
c, Å	7.1192(14)	7.8285(7)	7.9723(8)	18.7233(11)	8.6857(5)	11.0683(9)
α, deg	90	64.908(7)	73.897(9)	90	90	76.326(7)
β, deg	90.000(5)	65.418(8)	69.213(9)	104.242(7)	95.266(6)	79.414(7)
γ, deg	90	67.476(9)	63.009(10)	90	90	69.246(7)
V, Å^3	459.46(13)	317.57(5)	368.28(7)	1097.73(12)	876.75(9)	610.14(9)
Z	4	2	2	4	4	2
D_{calcd}, g cm^{-3}	1.72	1.91	1.98	1.73	1.85	1.71
$\mu(MoK\alpha)$, cm^{-1}	0.2	0.2	0.5	0.2	0.2	0.2
$F(000)$, e	248	188	224	592	504	326
hkl range	$-8 \leq 8$; $-12 \leq 8$; $-6 \leq 9$	$-8 \leq 7$; $-8 \leq 7$; $-9 \leq 9$	$-8 \leq 8$; $-9 \leq 9$; $-9 \leq 9$	$-11 \leq 10$; $-8 \leq 7$; $-23 \leq 23$	$-9 \leq 8$; $-16 \leq 15$; $-6 \leq 10$	$-9 \leq 7$; $-10 \leq 9$; $-13 \leq 13$
$((\sin\theta)/\lambda)_{max}$, Å^{-1}	27.0	26.5	26.0	26.5	26.0	26.5
Refl. measd./unique/R_{int}	2578/998/0.039	1879/1276/0.012	2805/1444/0.023	8692/2258/0.032	3807/1718/0.022	4257/2510/0.025
Param. refined	94	134	142	130	177	250
$R1$ (obs)^a	0.0358	0.0303	0.0323	0.0355	0.0319	0.0350
$wR2$ (all data)^b	0.0801	0.0855	0.0773	0.0967	0.0783	0.0639
GoF (F^2)^c	1.02	1.07	1.01	1.04	0.95	0.84
$\Delta\rho_{fin}$ (min/max), e Å^{-3}	−0.21/0.20	−0.26/0.27	−0.53/0.24	−0.45/0.38	−0.35/0.18	−0.26/0.19

^{a} $R1 = \Sigma||F_o| - |F_c||/\Sigma|F_o|$; ^{b} $wR2 = [\Sigma w(F_o^2 - F_c^2)^2 / \Sigma w(F_o^2)^2]^{1/2}$, $w = [\sigma^2(F_o^2) + (AP)^2 + BP]^{-1}$, where $P = (\text{Max}(F_o^2, 0) + 2F_c^2)/3$ and A and B are constants adjusted by the program; ^{c} GoF $= S = [\Sigma w(F_o^2 - F_c^2)^2/(n_{obs} - n_{param})]^{1/2}$, where n_{obs} is the number of data and n_{param} the number of refined parameters.

Atoms A–B	2	3	4	5	6	7
O1–N2	1.245(2)	1.239(1)	1.247(2)	1.235(2)	1.252(2)	1.247(2)
O2–N2	1.254(2)	1.236(1)	1.239(2)	1.240(2)	1.230(2)	1.243(2)
N1–N2	1.336(2)	1.348(2)	1.338(2)	1.345(2)	1.348(2)	1.343(2)
N3–N4	1.414(2)	1.411(2)	1.408(2)	1.414(2)	1.415(2)	1.421(2)
N1–C1	1.374(2)	1.346(2)	1.348(3)	1.354(2)	1.350(2)	1.355(2)
N3–C1	1.334(2)	1.348(2)	1.355(3)	1.356(2)	1.354(2)	1.351(2)
N5–C1	1.319(3)	1.320(2)	1.306(3)	1.314(2)	1.306(2)	1.312(2)

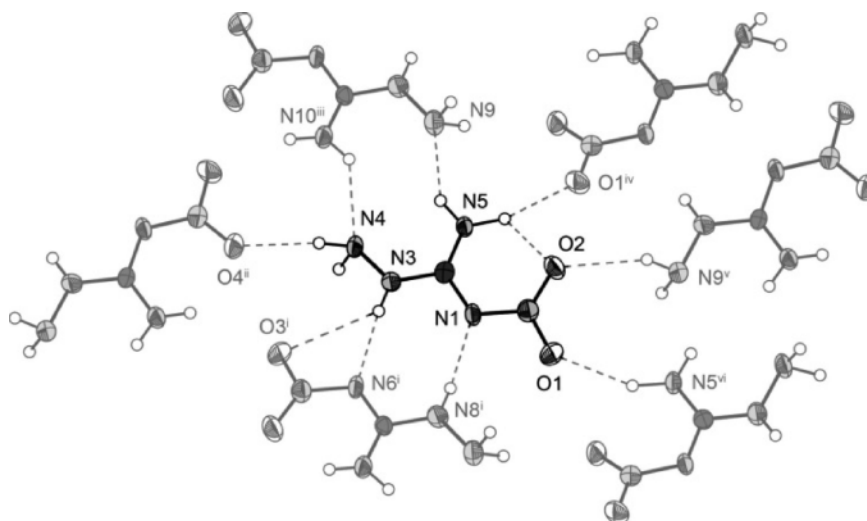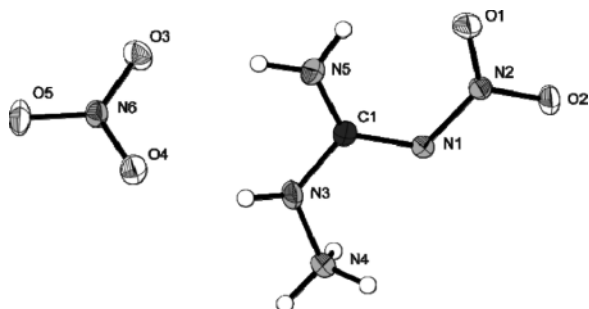Table 2. Selected bond lengths (Å) of compounds **2** – **7**.

Fig. 3. Hydrogen bonding of one aminonitroguanidine molecule. Symmetry codes: (i) $1 - x$, $1 - y$, $1 - z$; (ii) $1 + x$, $0.5 - y$, $0.5 + z$; (iii) $1 - x$, $-y$, $1 - z$; (iv) $1 - x$, $-0.5 + y$, $0.5 - z$; (v) x, $0.5 - y$, $-0.5 + z$; (vi) $1 - x$, $0.5 + y$, $0.5 - z$.

Fig. 4. Molecular structure of compound **3**. Ellipsoids are drawn at the 50 % probability level.
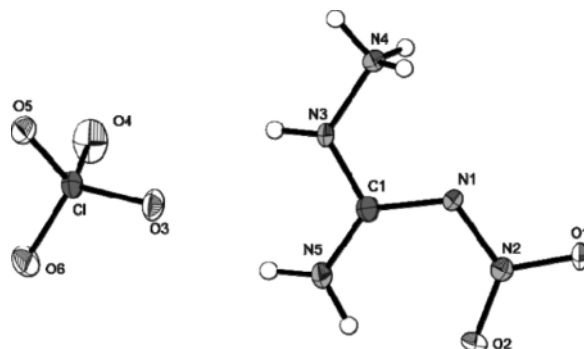

Fig. 5. Molecular structure of compound **4**. Ellipsoids are drawn at the 50 % probability level.

drogen bonds. **2** crystallizes in a layer-like structure, in which the layers are formed by the H-bond modes depicted in Fig. 3.

This constitution is observed for all ANQ salts presented in this work and is therefore probably caused by the protonation of nitrogen atom N4. The cations of compound **3** are arranged parallel and are connected by the nitrate anions which follow the direction of the hydrazinium proton H4c (not within the cation's plane). Fig. 4 shows the molecular moiety of compound **3**.

The perchlorate salt **4** crystallizes triclinically with the highest density $(1.98 \, \mathrm{g\,cm^{-3}})$ of the investigated compounds (Fig. 5). The Cl–O bond lengths in the ClO_4^- anion lie between 1.41 and 1.44 Å, which is a commonly observed bond length and can also be found in other perchlorate structures [20].

Single crystals of **5** were obtained from a water/ethanol mixture. Salt **5** holding monodeprotonated 5-nitriminotetrazolate as the counter anion could only
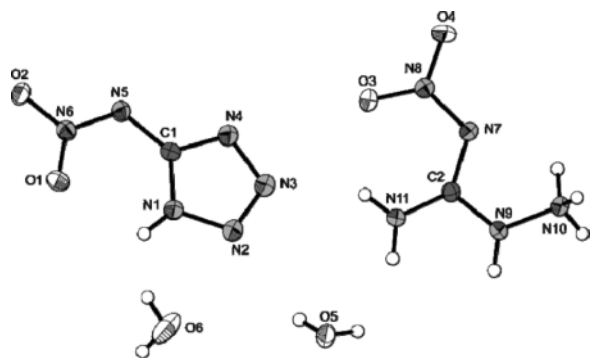
Fig. 6. Molecular structure of compound **5**. Ellipsoids are drawn at the 50 % probability level. Selected bond lengths of the nitriminotetrazolate anion (Å): O1–N6 1.245(2), O2–N6 1.269(2), N1–C1 1.340(2), N1–N2 1.349(2), N2–N3 1.294(2), N3–N4 1.354(2), N4–C1 1.332(2), N5–N6 1.318(2), N5–C1 1.376(2).
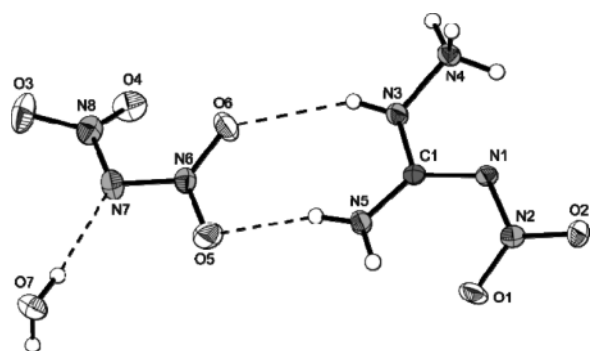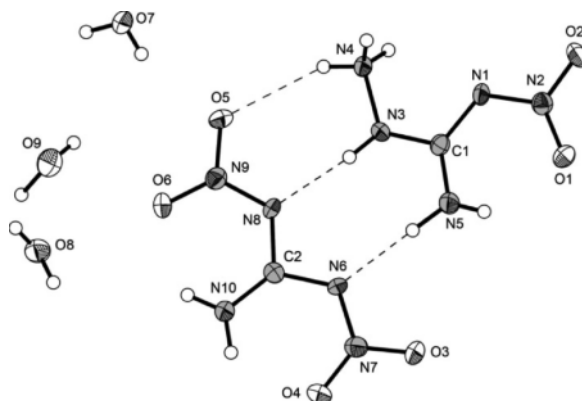

Fig. 8. Molecular structure of compound **7**. Ellipsoids are drawn at the 50 % probability level. Selected bond lengths of the DNQ anion (Å): O3–N7 1.2422(18), O4–N7 1.2430(17), O5–N9 1.2544(17), O6–N9 1.2491(18), N6–N7 1.3426(19), N6–C2 1.363(2), N8–N9 1.3316(19), N8–C2 1.376(2), N10–C2 1.309(2).

Fig. 7. Molecular structure of compound **6**. Ellipsoids are drawn at the 50 % probability level. Bond lengths of the dinitramide anion (Å): O3–N8 1.2317(17), O4–N8 1.2172(17), O5–N6 1.2541(16), O6–N6 1.2287(16), N6–N7 1.3423(17), N7–N8 1.3926(18).

be obtained in crystalline form (monoclinic space group $P2_1/c$) with the inclusion of two molecules of crystal water (Fig. 6). The planar structure of the anion, fixed by the intramolecular hydrogen bond N1–H1···O1 (graph set R1,1(6)), is in agreement with several examples published in the literature [21, 22] bearing this anion. The packing is best described by a wave-like arrangement along the *c* axis.

Amino-nitroguanidinium dinitramide monohydrate (**6**) crystallizes also in the monoclinic space group $P2_1/c$ with $Z = 4$ and a high density of 1.85 g cm^{-3}. The dinitramide anion participating in several strong hydrogen bonds is significantly twisted (bent angle ~59.5°) (Fig. 7). Again a wave-like arrangement along the *b* axis can be detected.

The combination of two different nitroguanidinines in compound **7** leads to the inclusion of two and a half crystal water molecules in the crystalline state (Fig. 8). The compound crystallizes in the triclinic space group $P\bar{1}$ with the lowest density of 1.705 g cm^{-3} observed in this work. The dinitroguanidinate anion follows the structure described for its ammonium salt [23]. In the packing layers are formed by the cations and anions. The parallel layers are exclusively connected by hydrogen bonds involving the crystal water molecules between the layers.

NMR spectroscopy

^{1}H as well as ^{13}C and ^{14}N NMR spectroscopy were applied to identify 1-amino-3-nitroguanidine and its salts. Additionally a ^{15}N NMR spectrum of **2** was recorded. For better comparison all spectra were measured using [D$_6$]DMSO as solvent, and all chemical shifts are given with respect to TMS (^{1}H, ^{13}C) and nitromethane (^{14}N/^{15}N). The proton spectrum of the neutral compound **2** reveals 4 singlets corresponding to the protons of the NH and of both NH$_2$ groups. The signal of the hydrazine NH$_2$ group appears at 4.64 ppm at highest field. For the two protons of the C-bonded amino group two distinct signals at 8.22 and 7.52 ppm are observed. This indicates hindered rotation around the C–N bond due to partial double bond character. The signal of the NH proton is found at 9.29 ppm and thus
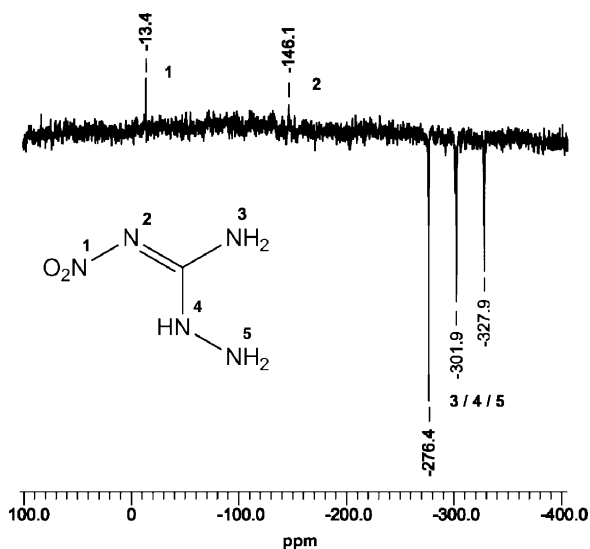
Fig. 9. $^{15}N\{^1H\}$ NMR spectrum of 1-amino-3-nitroguanidine (**2**).

at lowest field. The ^{13}C NMR spectrum shows a clear singlet at 161.5 ppm for the carbon atom, whereas the ^{14}N NMR spectrum reveals a singlet (line width at half height 17 Hz) at -13 ppm for the nitro group contained. The signals of the other nitrogen atoms are broad and difficult to locate in the ^{14}N NMR spectrum. However, they are clearly observed in the $^{15}N\{^1H\}$ NMR spectrum, which is shown in Fig. 9. Due to the nuclear Overhauser effect, the three nitrogen atoms having directly bonded protons display negative signals in the high-field region of the spectrum at -276.4, -301.8 and -327.9 ppm (NH/NH_2). In accordance with literature values of other primary nitramines [24], the signal at -146.3 ppm is assigned to the remaining nitrogen atom ($N–NO_2$) of the nitramine moiety.

All ionic compounds **3 – 7** show two broad singlets in their proton NMR spectra: one between 8.14 and 9.53 ppm for NH and a second between 6.90 and 8.38 ppm for $-NH_2/-NH_3{}^+$. In contrast to compound **2** only one signal is observed for the protons of the C-bonded amino group. In the carbon NMR spectra of compounds **3 – 7** one signal at 159.0 to 160.7 ppm can be assigned to the protonated aminonitroguanidine, and an additional signal at 154.7 ppm for deprotonated 5-nitriminotetrazole is observed in the spectrum of **5**. The ^{14}N NMR spectra show the signals of the nitro group of the aminonitroguanidinium cation at -15 ppm. Further nitro groups are observed

in the spectrum of **3** ($NO_3{}^-$, -7 ppm), **5** (NNO_2, -8 ppm), **6** ($N(NO_2)_2{}^-$, -10 ppm) and **7** (($NNO_2)_2$, -19 ppm). Also the protonated terminal amino groups of the cation can be detected as sharp signals at high field [-354 (**4**), -353 (**5**), -360 (**7**)].

Sensitivities and thermal stability

The impact sensitivity tests were carried out according to STANAG 4489 [25] modified instruction [26] using a BAM (Bundesanstalt für Materialforschung) drophammer [27]. The friction sensitivity tests were carried out according to STANAG 4487 [28] modified instruction [29] using the BAM friction tester. The classification of the tested compounds results from the "UN Recommendations on the Transport of Dangerous Goods" [30]. Additionally all compounds were tested for their sensitivity towards electrical discharge using the Electric Spark Tester ESD 2010 EN [31]. All sensitivities of compounds **2 – 7** were determined by the above described procedures. Expectedly, the perchlorate salt **4** is the most sensitive compound with values of 1 J (IS) and 20 N (FS), which has to be classified as very sensitive. Also the 5-nitriminotetrazolate **5** shows enhanced impact sensitivity (5 J) and friction sensitivity (96 N). The same applies to the friction sensitivity of the dinitramide **6** (40 N). Astonishingly, the impact sensitivity of **6** (10 J) is very similar to that of the nitrate salt **3** (10 J) and the dinitroguanidinate salt **7** (12 J). Regarding the impact sensitivity, the least sensitive compound within the investigated group is the unprotonated aminonitroguanidine itself. Apparently, protonation of the molecule leads to a certain destabilization by lowering the C–N bond order of the hydrazine moiety in aminonitroguanidine. The sensitivities towards electrical discharge are in a range between 0.10 J (**6**) and 0.50 J (**3**). These values depend strongly on the crystal size of the corresponding compound. The nitrate salt **3** crystallizes in large blocks, thus its sensitivity towards electrical discharge is comparatively low. The sensitivities as well as the decomposition and dehydration temperatures of all investigated compounds are gathered in Table 3.

Differential scanning calorimetry (DSC) measurements to determine the melting and decomposition temperatures of **2 – 7** (about 1.5 mg of each energetic material) were performed in covered Al containers with a hole in the lid at a nitrogen flow of 20 mL

Table 3. Sensitivities and thermal behavior of compounds **2–7**.

	IS (J)	FS (N)	ESD (J)	T_{dec} (°C)	T_{dehydr} (°C)
2	20	144	0.15	184	–
3	10	120	0.50	130	–
4	1	20	0.15	108	–
5	5	96	0.40	136	76
6	10	40	0.10	108	66
7	12	288	0.20	118	79

Table 4. CBS-4M results and gas phase enthalpies.

	Formula	$-H^{298}$ (a.u.)	$\Delta_{\text{f}}H$ (g) (kJ mol^{-1})
ANQ	$CH_5N_5O_2$	464.602726	161.7
ANQ$^+$	$CH_6N_5O_2{}^+$	464.914496	877.0
NO$_3{}^-$	$NO_3{}^-$	280.080446	−313.6
ClO$_4{}^-$	$ClO_4{}^-$	760.171182	−277.6
HAtNO$_2{}^-$	$CHN_6O_2{}^-$	516.973495	150.4
DN$^-$	$N_3O_4{}^-$	464.499549	−124.0
DNQ$^-$	$CH_2N_5O_4{}^-$	613.123393	−101.9

per minute on a Linseis PT 10 DSC [32] calibrated by standard pure indium and zinc at a heating rate of 5 °C min^{-1}. The most temperature-stable of the described energetic materials is the free base ANQ itself. It decomposes in a two step mechanism, which could be due to the loss of an amino group in a first step at 184 °C and then to the decomposition of the remaining nitroguanidine in a second step starting at 200 °C. For the ionic species **3–7** decomposition temperatures are significantly lower ranging from 108 °C (**4**, **6**) to 136 °C (**5**). The same arguments as for the sensitivities of the protonated aminonitroguanidine compounds can be applied to their thermal stability, which is the lowering of the C–N bond order resulting in an earlier decomposition. Additionally, the loss of crystal water in compounds **5–7** can be observed in the DSC curves as endothermic peaks between 66 °C (**6**) and 79 °C (**7**).

Heat of formation and detonation parameters

Heats and corresponding energies of formation were calculated with the atomization energy method (Eq. 1) using CBS-4M electronic energies (Table 4). Values obtained by this method have been shown to be suitable in several recently published studies [23].

CBS-4M energies of the atoms (C,H,N,O), ANQ, the ANQ$^+$ cation, and the anions were calculated with the GAUSSIAN09 (revision A1) software package [33] and checked for imaginary frequencies. Values for $\Delta_{\text{f}}H^\circ$ (atoms) were taken from the NIST database [34].

$$\Delta_{\text{f}}H^\circ_{(\text{g, M, 298})} = H_{(\text{Molecule, 298})} - \sum H^\circ_{(\text{Atoms, 298})} + \sum \Delta_{\text{f}}H^\circ_{(\text{Atoms, 298})} \quad (1)$$

For calculation of the solid-state energy of formation (Table 5) of **3–7**, the lattice energy (U_{L}) and lattice enthalpy (ΔH_{L}) were calculated from the corresponding molecular volumes (obtained from X-ray elucidations) according to the equations provided by Jenkins *et al.* [35]. With the calculated lattice enthalpy (Table 5) the gas-phase enthalpy of formation was converted into the solid-state (standard conditions) enthalpy of formation. These molar standard enthalpies of formation (ΔH_{m}) were used to calculate the molar solid state energies of formation (ΔU_{m}) according to Eq. 2 (Table 5):

$$\Delta U_{\text{m}} = \Delta H_{\text{m}} - \Delta nRT \quad (2)$$

with Δn being the change of moles of gaseous components.

Table 5. Solid state energies of formation ($\Delta_{\text{f}}U^\circ$) of compounds **2–7**.

	$\Delta_{\text{f}}H$ (g) (kJ mol^{-1})	V_{M} (nm^3)	U_{L} (kJ mol^{-1})	ΔH_{L} (kJ mol^{-1})	$\Delta_{\text{f}}H^\circ$ (s) (kJ mol^{-1})	Δn	$\Delta_{\text{f}}U^\circ$ (s) (kJ mol^{-1})	M (g mol^{-1})	$\Delta_{\text{f}}U^\circ$ (s) (kJ kg^{-1})
2	161.7	–	–	85.9[a]	76.9	6	91.8	119.1	770.4
3	563.4	0.158	537.8	541.2	22.2	8.5	43.3	182.1	237.5
4	599.4	0.184	591.3	594.8	4.6	8	24.5	219.6	111.4
5	544.3[b]	0.224	489.8	493.3	51.0	14	85.7	285.2	300.4
6	511.4	0.194	508.9	512.4	−0.2	11.5	27.5	244.1	112.7
7	40.9	0.243	480.0	484.4	−312.3	15.75	−273.3	313.09	−872.8

[a] Sublimation enthalpy calculated by Trouton's rule [36] ($188 \cdot T_{\text{m}}$ (K); $T_{\text{m}} = 457$ K); [b] values are corrected for hydrate water (−241 kJ mol^{-1} per water molecule).

Table 6. Energetic characteristics and calculated explosive performance parameters of compounds **2 – 7** using the EXPLO5 code.

	2	**3**	**4**	**5**	**6**	**7**
Formula	$CH_5N_5O_2$	$CH_6N_6O_5$	$CH_6N_5O_6Cl$	$C_2H_{11}N_{11}O_6$	$CH_8N_8O_7$	$C_2H_{13}N_{10}O_{8.5}$
FW, g mol^{-1}	119.08	182.10	219.54	285.18	244.12	313.19
N, % [a]	58.8	46.2	31.90	54.4	45.9	44.7
Ω, % [b]	−33.59	0.0	+10.93	−19.63	+6.55	−10.22
ρ, g cm^{-3} [c]	1.722	1.905	1.980	1.726	1.850	1.705
EXPLO5.04 values:						
$-\Delta_{Ex}U°$, kJ kg^{-1} [d]	4915	6191	–	5236	5636	5313
T_{det}, K [e]	3310	4196	–	3607	3949	3612
P_{CJ}, kbar [f]	307	427	–	317	377	311
V_{det}, m s^{-1} [g]	8729	9551	–	8753	9175	8656
V_o, L kg^{-1} [h]	878	857	–	880	871	890

[a] Nitrogen content; [b] oxygen balance [38]; [c] density from X-ray diffraction; [d] energy of explosion; [e] explosion temperature; [f] detonation pressure; [g] detonation velocity; [h] volume of detonation gases assuming only gaseous products.

The detonation parameters were calculated using the program EXPLO5 V5.04 [37]. The program is based on the steady-state model of equilibrium detonation and uses Becker-Kistiakowsky-Wilson's equation of state (BKW E. O. S.) for gaseous detonation products and Cowan-Fickett E. O. S. for solid carbon.

The calculations for **2 – 7** were performed using the maximum densities according to the crystal structures. Additionally the explosion performance parameters of the water-free dinitramide were calculated assuming the same density as for the monohydrate. Except for **6** and **7**, all calculated heats of formation are positive with values ranging from only slightly positive (**4**: 4.6 kJ mol^{-1}) to more endothermic (**2**: 76.9 kJ mol^{-1}). All calculated values for the heats and energies of formation can be found in Table 5.

Having a look at the explosive performance parameters shown in Table 6, the nitrate salt **3** and the dinitramide salt **6** stand out with their very high detonation velocities and pressures of 9551 m s^{-1} and 427 kbar (**3**) and 9175 m s^{-1} and 377 kbar (**6**), which are caused by their high densities of 1.91 g cm^{-3} (**3**) and 1.85 g cm^{-3} (**6**). The perchlorate salt **4** and dinitramide salt **6** reveal an even positive oxygen balance which is a desirable feature for oxidizers in propellant formulations. Compound **3** is an example of an energetic compound having a balanced oxygen content, which is found very rarely in the literature. Its combustion equation can be formulated ideally to be $CH_6N_6O_5 \rightarrow CO_2 + 3 H_2O + 3 N_2$. Also **2** shows a detonation velocity in the vicinity of 9000 m s^{-1} which is higher than commonly used RDX.

Valence bond (VB) calculations

In order to elucidate the bonding situation based on valence bond (VB) theory and to determine the most relevant Lewis-type structure(s), various calculations were performed using the VB2000 [version 2.5(R1)] code [39]. The input structure was taken from a fully optimized (within C_s symmetry) MP2/aug-cc-pVDZ calculation (NIMAG = 0) where all atoms involved in π bonding (O1, N2, O3, N4, C5, N6, N7) were placed into the *xy* plane (see Fig. 10), and the corresponding seven p_z orbitals were used as VB orbitals to accommodate the ten π electrons. In all VB calculations we used strictly localized p_z-π orbitals (BRILLMASK function in VB2000). For clarity, the π electrons are shown as dots (·) whereas the σ backbone (HF treatment) is shown as solid bonds (–) (Fig. 10).

Initially we carried out a CASVB(10,7)/D95 calculation using Dunning/Huzinaga's full double-zeta basis set and invoking resonance between all possible 196 π structures (NOROT option to disable any $\sigma - \pi$ mixing). The calculation clearly showed that only the seven structures (**I – VII**) shown in Fig. 10 contribute significantly to the resonance scheme (Hiberty weights > 0.01) (Table 7).

In a subsequent VB(10)/D95 calculation we only included the seven structures **I – VII** into the resonance scheme (Table 7). It is apparent that only structures **I – III** and **VI** have significant weight, whereas structures **IV**, **V** and **VII** are not significant contributors to the resonance scheme.

The above VB calculations reveal that resonance structures **I – III** and **VI** (Fig. 10) are the most rele-

	$-E$ (a.u.)	I	II	III	IV	V	VI	VII
CASVB(10,7)/D95	461.471657	0.04	0.29	0.05	0.02	0.01	0.07	0.06
VB(10)/D95	461.338488	0.07	0.70	0.07	0.02	0.01	0.11	0.02

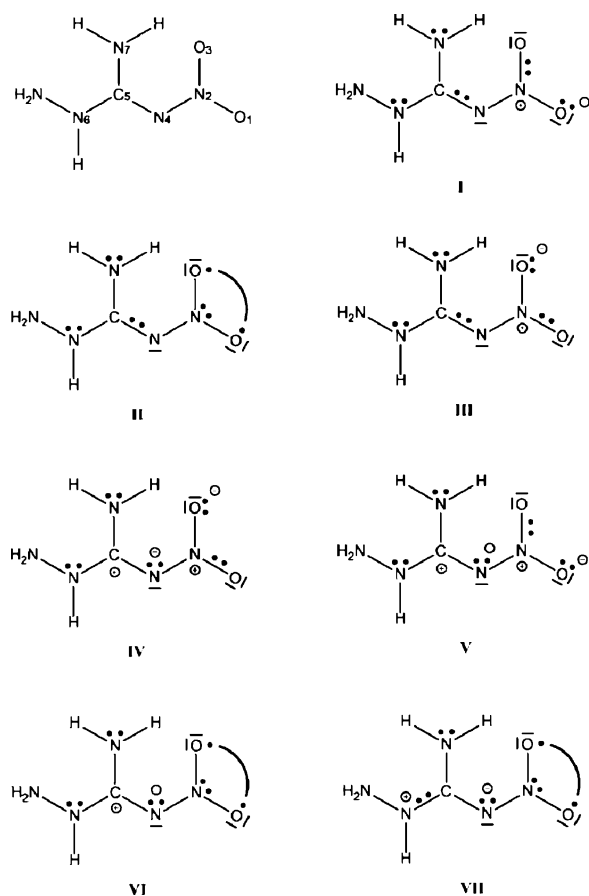Table 7. VB energies and Hiberty weights for resonance structures **I – VII** (see Fig. 10).

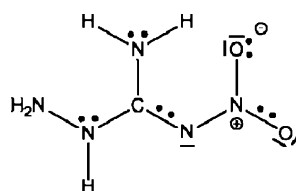Fig. 10. Atomic numbering and resonance structures **I – VII** for the π resonance scheme of **2**.

Fig. 11. Natural Lewis structure of ANQ (**2**).

pictures (VB and NBO) agree with a N4=C5 double bond and a strongly π-bound nitro ($-NO_2$) unit. It has to be stressed, however, that the natural Lewis structure is *not* a classical Lewis structure in the London-Heitler picture, and that the resonance structure **II** (see above) with one long (or Dewar-type) bond accounts best for maximizing the bond order and simultaneously reducing the number of formal charges.

Koenen Test of 1-amino-3-nitroguanidinium nitrate (3)

Due to its cheap and comparatively easy synthesis, 1-amino-3-nitroguanidinium nitrate (**3**) was investigated reguarding its explosion performance under confinement using a "Koenen test" steel sleeve apparatus [42, 43]. The performance of an explosive can be related to the data obtained from the Koenen test. Also the shipping classification of the substance can be determined, and the degree of venting required to avoid an explosion during processing operations can be evaluated. The explosive is placed in a non-reusable open-ended flanged steel tube, which is locked up with a closing plate with variable orifice (0 – 10 mm), through which gaseous decomposition products are vented. A defined volume of 25 mL of the compound is loaded into the flanged steel tube, and a threaded collar is slipped onto the tube from below. The closing plate is fitted over the flanged tube and secured with a nut. The explosion is initiated *via* thermal ignition using four Bunsen burners, which are lighted simultaneously. The test is completed when either rupture of the tube or no reaction is observed after heating the tube for a time period of at least 5 min. In case of the tube's rupture the fragments are collected and weighed. The reaction is evaluated as an explosion if the tube is destroyed into three or more pieces. The

vant individual structures for describing the π electron distribution of **2**. Whereas the Kekulé-type structures **I** and **III** have two π bonds each, the Kekulé-/Dewar-type structure **II** also with two π bonds (one Kekulé- and one Dewar-type bond) is by far the most important individual resonance structure for **2** since it does not carry any formal charge [40].

In addition, we also carried out an NBO analysis [41] and calculated the natural Lewis structure which is shown in Fig. 11. Taking into account that there is only one strong hyperconjugative interaction (LP (3) O3 → BD*(2) O1–N2) which essentially delocalizes the π bond between O1–N2 and O3–N2, both
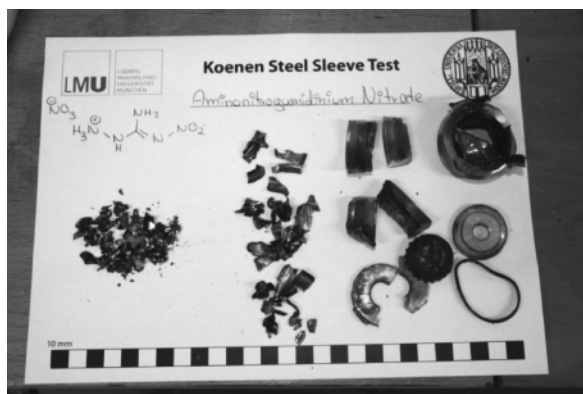
Fig. 12. Fragments of the steele sleeve after the ignition of 32.5 g 1-amino-3-nitroguanidinium nitrate (**3**).

Koenen test was performed with 32.5 g of 1-amino-3-nitroguanidinium nitrate (**3**) using a closing plate with an orifice of 10 mm. The first trial was successful as indicated by the rupture of the steel tube into approximately 100 pieces, the sizes of which are reaching from 40 mm down to smaller than 1 mm (Fig. 12). TNT destroys the steel tube up to an orifice width of 6 mm, RDX even up to 8 mm [44]. Compared to these commonly used secondary explosives, the detonation performance of **3** is apparently better, which is already indicated by the calculated performance data.

Conclusion

From the experimental study of energetic materials based on 1-amino-3-nitroguanidine the following conclusions can be drawn:

– 3-Amino-1-nitroguanidine can be easily prepared by the reaction of 1-nitroguanidine and hydrazine hydrate.
– 1-Amino-3-nitroguanidine can be protonated using moderate to strong "Brønsted acids" such as nitric acid, hydrochloric acid, perchloric acid, dinitroguanidine, or 5-nitriminotetrazole.
– The hydrochloride of 1-amino-3-nitroguanidine can be utilized in metathesis reactions with silver salts of nitrogen/oxygen-rich anions. The metathesis was used for the synthesis of 1-amino-3-nitroguanidinium dinitramide.
– The crystal structures of compounds **2**–**7** were determined using low-temperature single-crystal X-ray diffraction.

– A comprehensive characterization of the physicochemical properties and sensitivities of compounds **2**–**7** is given. Promising detonation parameters were calculated especially for **3** compared to common explosives like TNT and RDX. The outstanding performance (calculated values: $p_{CJ} = 427$ kbar; $D = 9551$ m s^{-1}) qualifies it for further investigations concerning special military applications. Unfortunately the decomposition temperatures of the protonated species are low compared to the free base 1-amino-3-nitroguanidine. This causes major restrictions for the investigated compounds with respect to their application as secondary explosives.

Experimental Section

Caution! ANQ and its salts are highly energetic materials with increased sensitivities towards shock and friction. Therefore, proper safety precautions (safety glass, face shield, earthed equipment and shoes, Kevlar® gloves and ear plugs) have to be applied while synthesizing and handling the described compounds.

All chemicals and solvents were employed as received (Sigma-Aldrich, Fluka, Acros). ^{1}H and ^{13}C spectra were recorded using Jeol Eclipse 270, Jeol EX 400 or Jeol Eclipse 400 instruments. The chemical shifts quoted in ppm in the text refer to typical standards such as tetramethylsilane (^{1}H, ^{13}C) or nitromethane (^{14}N/^{15}N). To determine the melting and decomposition temperatures of the described compounds a Linseis PT 10 DSC (heating rate 5 °C min^{-1}) was used. Infrared spectra were measured using a Perkin Elmer Spectrum One FT-IR spectrometer as KBr pellets. Raman spectra were recorded on a Bruker MultiRAM Raman Sample Compartment D418 equipped with an Nd-YAG Laser (1064 nm) and an LN-Ge diode as detector. Mass spectra of the described compounds were measured at a Jeol MStation JMS 700 using FAB technique. To measure elemental analyses, a Netsch STA 429 simultaneous thermal analyzer was employed.

1-Amino-3-nitroguanidine (2)

Commercially available nitroguanidine (25 g, 192 mmol) is dispensed in 250 mL of water, and the mixture is heated to 55 °C. Hydrazine hydrate (10.5 mL, 216 mmol) is added dropwise over a period of 15 min, and the temperature is kept at 55 °C for further 15 min under constant stirring. After the mixture has turned to a clear, orange solution, it is cooled to room temperature in an ice bath, and the reaction is quenched with conc. hydrochloric acid (pH = 7). 1-Amino-3-nitroguanidine starts to precipitate after the solution has been cooled to 4 °C overnight. The product is separated by suction filtration and recrystallized from hot water. Yield: 10.3 g (86 mmol, 45 %). – DSC (5 °C min^{-1}):

184 °C (dec. 1), 200 °C (dec. 2). – IR (KBr, cm^{-1}): $\tilde{\nu}$ = 3551 (s), 3411 (s), 3234 (s), 2025 (w), 1692 (m), 1637 (s), 1616 (vs), 1545 (m), 1502 (m), 1443 (m), 1384 (m), 1329 (m), 1134 (m), 1108 (m), 1088 (m), 1031 (m), 1005 (w), 963 (w), 870 (w), 772 (w), 745 (w), 696 (w), 622 (m), 571 (w), 482 (m). – Raman (1064 nm, 200 mW, 25 °C, cm^{-1}): $\tilde{\nu}$ = 3319 (4), 3255 (13), 1659 (5), 1616 (4), 1580 (32), 1381 (13), 1287 (32), 1190 (5), 1111 (39), 1019 (5), 961 (100), 770 (27), 483 (30), 419 (33), 378 (10), 248 (13). – ^{1}H NMR ([D$_6$]DMSO, 25 °C, ppm): δ = 9.29 (s, 1 H, NH), 8.23 (s, 1H, C-NH_AH$_B$), 7.52 (s, 1H, C-N$H_A$$H_B$), 4.64 (s, 2H, N-NH$_2$). – ^{13}C NMR ([D$_6$]DMSO, 25 °C, ppm): δ = 161.5 (*C*(NNO$_2$)(N$_2$H$_4$)(NH$_2$)). – ^{15}N NMR ([D$_6$]DMSO, 25 °C, ppm): δ = –13.3 (*N*O$_2$), –146.3 (*N*NO$_2$), –276.4 (*N*H/*N*H$_2$), –301.8 (*N*H/*N*H$_2$), –327.9 (*N*H/*N*H$_2$). – MS ((–)-FAB): m/z = 117.99 [M–H]$^-$. – CH$_5$N$_5$O$_2$ (119.08): calcd. C 10.09, H 4.23, N 58.81%; found C 10.51, H 4.32, N 58.90%. – BAM drophammer: 20 J. – Friction tester: 144 N. – ESD: 0.15 J (at grain size 100 – 500 μm).

1-Amino-3-nitroguanidinium nitrate (3)

2 (5.00 g, 42.0 mmol) is dissolved in warm nitric acid (40%, 12.71 g, 84.0 mmol). The yellowish, clear solution is left for crystallization. **3** crystallizes in large, colorless blocks after a few hours (yield: 7.12 g, 39.1 mmol, 93%). – DSC (5 °C min^{-1}): 130 °C (dec.). – IR (KBr, cm^{-1}): $\tilde{\nu}$ = 3397 (m), 3293 (m), 3090 (m), 1648 (s), 1581 (s), 1470 (s), 1384 (vs), 1281 (vs), 1215 (s), 1166 (m), 1112 (m), 1050 (w), 1014 (w), 913 (w), 823 (w), 785 (w), 708 (w), 625 (w), 568 (w). – Raman (1064 nm, 500 mW, 25 °C, cm^{-1}): $\tilde{\nu}$ = 3319 (2), 3046 (2), 1623 (8), 1578 (11), 1494 (6), 1373 (4), 1263 (37), 1218 (9), 1168 (7), 1053 (100), 1010 (6), 921 (12), 803 (20), 788 (4), 735 (4), 712 (4), 626 (20), 440 (9), 358 (18), 256 (14), 173 (16), 112 (9). – ^{1}H NMR ([D$_6$]DMSO, 25 °C, ppm): δ = 9.53 (s, 5 H, NH$_2$), 8.38 (s, 1H, N*H*-NH$_2$). – ^{13}C NMR ([D$_6$]DMSO, 25 °C, ppm): δ = 159.3 (*C*(NNO$_2$)(N$_2$H$_4^+$)(NH$_2$)). – ^{14}N NMR ([D$_6$]DMSO, 25 °C, ppm): δ = –7 (*N*O$_2$), –15 (*N*O$_3$). – MS ((+)-FAB): m/z = 120 [C(NNO$_2$)(NH$_2$)(NHNH$_3$)]$^+$. – MS ((–)-FAB): m/z = 62 [NO$_3$]$^-$. – CH$_6$N$_6$O$_5$ (182.04): calcd. C 6.60, H 3.32, N 46.15%; found C 6.49, H 3.30, N 45.82%. – BAM drophammer: 10 J. – Friction tester: 120 N (neg.). – ESD: 0.5 J (at grain size 500 – 1000 μm).

1-Amino-3-nitroguanidinium perchlorate (4)

2 (1.19 g, 10 mmol) is dissolved in 1M HClO$_4$ (20 mL, 20 mmol) under moderate heating to 60 °C. **4** crystallizes from the clear solution in colorless blocks. Yield: 4.16 g, 18.9 mmol, 95%). – DSC (5 °C min^{-1}): 108 °C (dec.). – IR (ATR, cm^{-1}): $\tilde{\nu}$ = 3387 (m), 3293 (m), 3084 (m, br), 3008 (m, br), 2891 (m, br), 2753 (m, br), 2686 (m, br), 2168 (w), 1705 (m), 1634 (m), 1559 (m), 1484 (m), 1450 (m), 1373 (m, br), 1270 (m, br), 1089 (vs, br), 1019 (s, br), 930 (s), 785 (m), 687 (w). – Raman (1064 nm, 400 mW, 25 °C, cm^{-1}): $\tilde{\nu}$ = 3336 (3), 1623 (6), 1572 (10), 1491 (14), 1264 (28), 1159 (9), 1107 (10), 1038 (4), 1001 (11), 933 (100), 799 (25), 634 (35), 472 (15), 453 (17), 436 (8), 359 (32), 285 (9). – ^{1}H NMR ([D$_6$]DMSO, 25 °C, ppm): δ = 9.03 (s, NH-NH$_3^+$), 8.37 (s, NH$_2$). – ^{13}C NMR ([D$_6$]DMSO, 25 °C, ppm): δ = 159.0 (*C*(NNO$_2$)(N$_2$H$_4^+$)(NH$_2$)). – MS ((+)-FAB): m/z =120.1 [C(NNO$_2$)(N$_2$H$_3$)(NH$_2$)+H]$^+$. – MS ((–)-FAB): m/z = 98.9 [ClO$_4$]$^-$. – CH$_6$ClN$_5$O$_6$ (219.54): calcd. C 5.47, H 2.75, N 31.90%; found C 5.70, H 2.80, N 31.28%. – BAM drophammer: 1 J. – Friction tester: 20 N. – ESD: 0.15 J (at grain size 100 – 500 μm).

1-Amino-3-nitroguanidinium 5-nitriminotetrazolate dihydrate (5)

2 (1.19 g, 10 mmol) is dissolved in a few milliliters of boiling water. The solution is cooled to 70 °C, and then a solution of 5-nitriminotetrazole (1.63 g, 11 mmol) is added slowly. The solvent is removed *in vacuo* and the residue recrystallized from an ethanol/water mixture. Yield: 2.17 g (7.6 mmol, 76%). – DSC (5 °C min^{-1}): 136 °C (dec.). – IR (KBr, cm^{-1}): $\tilde{\nu}$ = 3358 (vs), 3126 (s), 2939 (s), 2736 (s, br), 1658 (s), 1591 (s), 1531 (s), 1489 (s), 1436 (s), 1384 (s), 1313 (s), 1267 (s) 1210 (s), 1167 (m), 1144 (m), 1117 (m), 1087 (m), 1042 (s), 918 (w), 870 (w), 789 (w), 738 (w), 638 (m), 489 (w), 457 (w). – Raman (1064 nm, 300 mW, 25 °C, cm^{-1}): $\tilde{\nu}$ = 3908 (2), 3701 (2), 3355 (3), 3106 (3), 1581 (2), 1534 (100), 1437 (2), 1382 (3), 1315 (25), 1272 (6), 1144 (5), 1030 (34), 1010 (16), 925 (5), 874 (4), 799 (5), 757 (3), 630 (5), 457 (3), 415 (3), 376 (2), 251 (3), 113 (4), 85 (31). – ^{1}H NMR ([D$_6$]DMSO, 25 °C, ppm): δ = 8.15 (s, NH), 7.13 (NH$_2$). – ^{13}C NMR ([D$_6$]DMSO, 25 °C, ppm): δ = 160.7 (*C*(NNO$_2$)(N$_2$H$_4^+$)(NH$_2$)), 154.7 (*C*N$_4$). – MS ((+)-FAB): m/z = 120.2 [C(NNO$_2$)(N$_2$H$_4$)(NH$_2$)]$^+$. – MS ((–)-FAB): m/z = 129.1 [HATNO$_2$]$^-$. – C$_2$H$_{11}$N$_{11}$O$_6$(281.15): calcd. C 8.42, H 3.89, N 54.03%; found C 8.51, H 3.85, N 54.01%. – BAM drophammer: 5 J. – Friction tester: 96 N. – ESD: 0.4 J (at grain size 100 – 500 μm).

1-Amino-3-nitroguanidinium dinitramide monohydrate (6)

10 mmol of silver dinitramide acetonitrile adduct was prepared according to the literature [9]. 1-Amino-3-nitroguanidinium chloride (1.47 g, 9.4 mmol) is dissolved in 10 mL of boiling water. After cooling the solution to about 60 °C, the silver dinitramide acetonitrile adduct, dissolved in 5 mL of acetonitrile is added dropwise to the solution. After complete addition, the mixture is stirred under the exclusion of light at 35 °C for further 2 h. The mixture is cooled to 5 °C in a refrigerator and then filtered. **6** crystallizes from the clear filtrate in colorless blocks. Yield: 1.34 g (5.5 mmol, 59%). – DSC (5 °C min^{-1}): 66 °C (dehydr.), 108 °C (dec.). – IR

(ATR, cm^{-1}): $\tilde{\nu}$ = 3535 (w), 3413 (m), 3296 (m), 3121 (m), 2736 (m), 1633 (m), 1579 (m), 1508 (m), 1467 (m), 1429 (m), 1387 (m), 1324 (w), 1265 (m), 1167 (s), 1037 (m), 994 (m), 905 (m), 823 (w), 783 (w), 760 (m), 740 (w). – Raman (1064 nm, 400 mW, 25 °C, cm^{-1}): $\tilde{\nu}$ = 3333 (4), 3133 (4), 1574 (24), 1528 (20), 1491 (27), 1426 (17), 1397 (23), 1340 (90), 1331 (84), 1320 (100), 1258 (78), 1199 (19), 1182 (22), 1161 (21), 1105 (6), 1035 (45), 993 (11), 964 (31), 920 (40), 826 (95), 805 (54), 762 (12), 622 (43), 497 (44), 442 (23), 362 (21), 316 (12), 298 (16), 252 (7). – ^{1}H NMR ([D$_6$]DMSO, 25 °C, ppm): δ = 8.37 (s, 1H, NH), 6.90 (s, 5H, -NH$_2$, -NH$_3{}^+$). – ^{13}C NMR ([D$_6$]DMSO, 25 °C, ppm): δ = 159.2 (C(NNO$_2$)(N$_2$H$_4{}^+$)(NH$_2$)). –^{14}N NMR ([D$_6$]DMSO, 25 °C, ppm): δ = −10 (N(NO_2)$_2$), −15 (N-NO_2). – MS ((+)-FAB): m/z = 119.9 [C(NNO$_2$)(N$_2$H$_3$)(NH$_2$)+H]$^+$. – MS ((−)-FAB): m/z = 106.1 [N(NO$_2$)$_2$]$^-$. – CH$_8$N$_8$O$_7$(244.12): calcd. C 4.92, H 3.30, N 45.90 %; found C 4.74, H 3.23, N 44.40 %. – BAM drophammer: 10 J. – Friction tester: 40 N. – ESD: 0.10 J (at grain size 500 – 1000 μm).

1-Amino-3-nitroguanidinium dinitroguanidinate pentahemihydrate (7)

Dinitroguanidine (1.49 g, 10 mmol) is dissolved in 10 mL of hot water and poured onto neat **2** (1.19 g, 10 mmol). The suspension is heated until no precipitate is observed any more and then filtered. The filtrate shows evolution of gas and turns to light yellow. A yellow, amorphous precipitate starts to form, which is filtered off again. From the mother liquor, **7** precipitates in colorless blocks on standing for a few minutes. Yield: 1.85 g (5.9 mmol, 59 %). – DSC

(5 °C min^{-1}): 79 °C (dehydr.), 118 °C (dec.). – IR (KBr, cm^{-1}): $\tilde{\nu}$ = 3605 (m), 3409 (s), 3377 (s), 3205 (m), 2672 (m), 1619 (s), 1492 (m), 1384 (m), 1357 (m), 1259 (vs), 1218 (vs), 1150 (m), 1112 (m), 1063 (m), 974 (w), 915 (w), 785 (m), 764 (w), 720 (w), 680 (m), 636 (m), 589 (w), 550 (w). – Raman (1064 nm, 500 mW, 25 °C, cm^{-1}): $\tilde{\nu}$ = 3440 (5), 3199 (9), 1609 (15), 1578 (15), 1456 (22), 1370 (38), 1310 (5), 1254 (19), 1191 (35), 1154 (100), 1060 (24), 977 (54), 917 (8), 792 (32), 631 (14), 553 (22), 554 (6), 352 (24), 231 (13). – ^{1}H NMR ([D$_6$]DMSO, 25 °C, ppm): δ = 9.74 (s), 9.52 (s), 8.59 (s), 8.14 (s), 5.30 (s). – ^{13}C NMR ([D$_6$]DMSO, 25 °C, ppm): δ = 161.4 (C(NNO$_2$)(N$_2$H$_3$)(NH$_2$)), 160.3 (C(NNO$_2$)(N$_2$H$_4{}^+$)(NH$_2$)), 159.5 (C(NH$_2$)(N-NO$_2$)$_2$). – ^{14}N NMR ([D$_6$]DMSO, 25 °C, ppm): δ = −15 (CNNO_2), −19 (C(NNO_2)$_2$). – MS ((+)-FAB): m/z = 120.1 [C(NNO$_2$)(N$_2$H$_4$)(NH$_2$)]$^+$. – MS ((−)-FAB): m/z = 147.9 [C(NH$_2$)(N-NO$_2$)$_2$]$^-$. – C$_2$H$_{13}$N$_{10}$O$_{8.5}$ (313.09): calcd. C 7.67, H 4.18, N 44.72 %; found C 7.90, H 4.20, N 45.43 %. – BAM drophammer: 12 J. – Friction tester: 288 N. – ESD: 0.20 J (at grain size 100 – 500 μm).

[1] A. W. Hofmann, *J. Chem. Soc. Trans.* **1866**, *19*, 249 – 255.

[2] a) R. G. S. Berlinck, A. C. B. Burtoloso, A. E. Trindade-Silva, S. Romminger, R. P. Morais, K. Bandeira, C. M. Mizuno, *Nat. Prod. Rep.* **2010**, *27*, 1871 – 1907; b) F. Saczewski, L. Balewski, *Expert Opin. Ther. Pat.* **2009**, *19*, 1417 – 1448.

[3] T. E. O'Connor, K. Horgan and J. Reilly, *J. Appl. Chem.* **1951**, *1*, 91 – 92.

[4] a) L. Jousselin, *Compt. Rend.* **1879**, *88*, 1086; b) G. Pellizzari, *Gazz. Chim. Ital.* **1891**, *21*, 405 – 409.

[5] A. A. Astrat'yev, D. V. Dashko, L. L. Kuznetsov, *Russ. J. Org. Chem.* **2003**, *3*, 501 – 512.

[6] C. Gonzalez, G. Ballester, M. A. Rodriguez, 40th International Annual Conference of ICT (Energetic Materials), **2009**, 44/1 – 44/11.

[7] J. A. Castillo-Meléndez, B. T. Golding, *Synthesis* **2004**, *10*, 1655 – 1663.

[8] R. A. Henry, H. D. Lewis, G. B. L. Smith, *J. Am. Chem. Soc.* **1950**, *72*, 2015.

[9] R. Phillips, J. F. Williams, *J. Am. Chem. Soc.* **1928**, *50*, 2465.

[10] A. F. McKay, *Chem. Rev.* **1952**, *51*, 301 – 346.

[11] J. Stierstorfer, T. M. Klapötke, *Helv. Chim. Acta* **2007**, *90*, 2132 – 2150.

[12] T. M. Klapötke, B. Krumm, M. Scherr, *Dalton Trans.* **2008**, *43*, 5876 – 5878.

[13] CRYSALISPRO (version 1.171.35.11), Agilent Technologies, Loveland, Colorado (USA) **2011**.

[14] a) G. M. Sheldrick, SHELXS-97, Program for the Solution of Crystal Structures, University of Göttingen, Göttingen (Germany) **1997**. See also: G. M. Sheldrick, *Acta Crystallogr.* **1990**, *A46*, 467 – 473; b) A. Altomare, G. Cascarano, C. Giacovazzo, A. Gugliardi, M. C. Burla, G. Polidori, M. Camalli, SIR92, A Program for Automatic Solution of Crystal Structures

by Direct Methods; see: A. Altomare, G. Cascarano, C. Giacovazzo, A. Gugliardi, M. C. Burla, G. Polidori, M. Camalli, *J. Appl. Crystallogr.* **1994**, *27*, 435; A. Altomare, G. Cascarano, C. Giacovazzo, A. Guagliardi, *J. Appl. Crystallogr.* **1993**, *26*, 343 – 350.

[15] G. M. Sheldrick, SHELXL-97, Program for the Refinement of Crystal Structures, University of Göttingen, Göttingen (Germany) **1997**. See also: G. M. Sheldrick, *Acta Crystallogr.* **2008**, *A64*, 112 – 122.

[16] A. L. Spek, PLATON, A Multipurpose Crystallographic Tool, Utrecht University, Utrecht (The Netherlands) **2010**. See also: A. L. Spek, *J. Appl. Crystallogr.* **2009**, *D65*, 148 – 155.

[17] L. J. Farrugia, WINGX, A MS-Windows System of Programs for Solving, Refining and Analysing Single Crystal X-ray Diffraction Data for Small Molecules, University of Glasgow, Glasgow, Scotland (UK) **2005**. See also: L. J. Farrugia, *J. Appl. Crystallogr.* **1999**, *32*, 837 – 838.

[18] CCDC 831494 (**2**), 831496 (**3**), 831492 (**4**), 831491 (**5**), 831493 (**6**), and 831495 (**7**) contain the supplementary crystallographic data for this paper. These data can be obtained free of charge from The Cambridge Crystallographic Data Centre *via* www.ccdc.cam.ac.uk/data_request/cif.

[19] S. R. Naidu, N. M. Bhide, K. V. Prabhakaran, E. M. Kurian, *J. Thermal Anal.* **1995**, *44*, 1449 – 1462.

[20] A. Martin, A. A. Pinkerton, *Acta Crystallogr.* **1996**, *C52*, 1048 – 1052.

[21] N. Fischer, T. M. Klapötke, D. Piercey, S. Scheutzow, J. Stierstorfer, *Z. Anorg. Allg. Chem.* **2010**, *636*, 2357 – 2363.

[22] T. M. Klapötke, J. Stierstorfer, B. Weber, *Inorg. Chim. Acta* **2009**, *362*, 2311 – 2320.

[23] T. Altenburg, T. M. Klapötke, A. Penger, J. Stierstorfer, *Z. Anorg. Allg. Chem*. **2010**, *636*, 463 – 471.

[24] J. Stierstorfer, T. M. Klapötke, A. U. Wallek, *Chem. Mater.* **2008**, *20*, 4519 – 4530.

[25] NATO standardization agreement (STANAG) on explosives, impact sensitivity tests, no. 4489, 1st ed., September 17, **1999**.

[26] WIWEB-Standarbeitsanweisung 4 – 5.1.02, Ermittlung der Explosionsgefährlichkeit, hier der Schlagempfindlichkeit mit dem Fallhammer, Nov. 8, **2002**.

[27] http://www.bam.de (retrieved April 2, **2012**).

[28] NATO standardization agreement (STANAG) on explosive, friction sensitivity tests, no. 4487, 1st ed., Aug. 22, **2002**.

[29] WIWEB-Standarbeitsanweisung 4 – 5.1.03, Ermittlung der Explosionsgefährlichkeit oder der Reibeempfindlichkeit mit dem Reibeapparat, Nov. 8, **2002**.

[30] Impact: insensitive > 40 J, less sensitive > 35 J, sensitive > 4 J, very sensitive < 3 J. Friction: insensitive $>$

360 N, less sensitive $= 360$ N, sensitive < 360 N and > 80 N, very sensitive < 80 N, extremely sensitive < 10 N. According to the UN Recommendations on the Transport of Dangerous Goods, (+) indicates not safe for transport.

[31] http://www.ozm.cz (retrieved April 2, **2012**).

[32] http://www.linseis.com (retrieved April 2, **2012**).

[33] M. J. Frisch, G. W. Trucks, H. B. Schlegel, G. E. Scuseria, M. A. Robb, J. R. Cheeseman, G. Scalmani, V. Barone, B. Mennucci, G. A. Petersson, H. Nakatsuji, M. Caricato, X. Li, H. P. Hratchian, A. F. Izmaylov, J. Bloino, G. Zheng, J. L. Sonnenberg, M. Hada, M. Ehara, K. Toyota, R. Fukuda, J. Hasegawa, M. Ishida, T. Nakajima, Y. Honda, O. Kitao, H. Nakai, T. Vreven, J. A. Montgomery Jr., J. E. Peralta, F. Ogliaro, M. Bearpark, J. J. Heyd, E. Brothers, K. N. Kudin, V. N. Staroverov, R. Kobayashi, J. Normand, K. Raghavachari, A. Rendell, J. C. Burant, S. S. Iyengar, J. Tomasi, M. Cossi, N. Rega, J. M. Millam, M. Klene, J. E. Knox, J. B. Cross, V. Bakken, C. Adamo, J. Jaramillo, R. Gomperts, R. E. Stratmann, O. Yazyev, A. J. Austin, R. Cammi, C. Pomelli, J. W. Ochterski, R. L. Martin, K. Morokuma, V. G. Zakrzewski, G. A. Voth, P. Salvador, J. J. Dannenberg, S. Dapprich, A. D. Daniels, Ö. Farkas, J. B. Foresman, J. V. Ortiz, J. Cioslowski, D. J. Fox, GAUSSIAN 09 (revision A.1), Gaussian, Inc., Wallingford CT (USA) **2009**.

[34] P. J. Linstrom, W. G. Mallard (Eds.), *NIST Chemistry WebBook*, NIST Standard Reference Database Number 69, National Institute of Standards and Technology, Gaithersburg MD, **2005**; http://webbook.nist.gov (retrieved October 27, **2011**).

[35] a) H. D. B. Jenkins, H. K. Roobottom, J. Passmore, L. Glasser, *Inorg. Chem.* **1999**, *38*, 3609 – 3620; b) H. D. B. Jenkins, D. Tudela, L. Glasser, *Inorg. Chem.* **2002**, *41*, 2364 – 2367.

[36] a) M. S. Westwell, M. S. Searle, D. J. Wales, D. H. Williams, *J. Am. Chem. Soc*. **1995**, *117*, 5013 – 5015; b) F. Trouton, *Philos. Mag.* **1884**, *18*, 54 – 57.

[37] M. Sueska, EXPLO5.04 program, Zagreb (Croatia) **2010**.

[38] Calculation of oxygen balance: $\Omega(\%) = (w\,O - 2x\,C - 1/2y\,H - 2z\,S) \cdot 1600 / M$ (w: number of oxygen atoms, x: number of carbon atoms, y: number of hydrogen atoms, z: number of sulfur atoms).

[39] J. Li, B. Duke, R. McWeeny, VB2000 (version 2.1), SciNet Technologies, San Diego, CA (USA) **2011**; http://www.scinetec.com/ (retrieved April 2, **2012**). See also: J. Li, R. McWeeny, *Int. J. Quantum Chem*. **2002**, *89*, 208 – 216.

[40] a) R. D. Harcourt, T. M. Klapötke, *Research Trends Inorg. Chem.* **2006**, *9*, 11 – 22; and references therein;

b) R. D. Harcourt, *Qualitative Valence-Bond Descriptions of Electron-Rich Molecules: Pauling "3-Electron Bonds" and "Increased-Valence Theory"*, Lecture Notes in Chemistry, Vol. 30, Springer, Berlin, Heidelberg, New York, **1982**; c) R. D. Harcourt, *Eur. J. Inorg. Chem.* **2000**, 1901–1916; d) T. M. Klapötke, A. Schulz with an invited chapter by R. D. Harcourt, *Quantum Chemical Methods in Main-Group Chemistry*, J. Wiley, Chichester, **1998**; e) T. M. Klapötke, Nichtmetallchemie, in *Moderne Anorganische Chemie*, (Ed.: E. Riedel), 3rd ed., Walter de Gruyter, Berlin, New York, **2007**.

[41] a) J. E. Carpenter, F. Weinhold, *J. Mol. Struct. (Theochem.)* **1988**, *169*, 41; b) J. P. Foster, F. Weinhold, *J. Am. Chem. Soc.* **1980**, *102*, 7211; c) A. E. Reed, F. Weinhold, *J. Chem. Phys.* **1983**, *78*, 4066; d) A. E. Reed, F. Weinhold, *J. Chem. Phys.* **1983**, 1736; e) A. E. Reed, R. B. Weinstock, F. Weinhold, *J. Chem. Phys.* **1985**, *83*, 735; f) A. E. Reed, L. A. Curtiss, F. Weinhold, *Chem. Rev.* **1988**, *88*, 899; g) F. Weinhold, J. E. Carpenter, *Plenum* **1988**, 227.

[42] R. C. West, S. M. Selby, *Handbook of Chemistry and Physics,* 48th ed., The Chemical Rubber Co., Cleveland, **1967**, pp. D22–D51.

[43] V. A. Ostrovskii, M. S. Pevzner, T. P. Kofman, I. V. Tselinskii, *Targets Heterocycl. Syst.* **1999**, *3*, 467.

[44] J. Köhler, R. Meyer, *Explosivstoffe*, 9th ed., Wiley-VCH, Weinheim, **1998**, pp. 166–168.